Molecular Plant Pathology

MOLECULAR PLANT PATHOLOGY (2018) 19(6), 1414–1426 DOI: 10.1111/mpp.12624

Disruption of calcineurin catalytic subunit (*cnaA*) in *Epichloë festucae* induces symbiotic defects and intrahyphal hyphae formation

MILENA MITIC[1,2], DANIEL BERRY[1], EMMA BRASELL[1], KIMBERLY GREEN[1,2], CAROLYN A. YOUNG[3], SANJAY SAIKIA[1], JASNA RAKONJAC[1] AND BARRY SCOTT[1,2,*]

[1]Institute of Fundamental Sciences, Massey University, Palmerston North 4442, New Zealand
[2]BioProtection Research Centre, Massey University, Palmerston North 4442, New Zealand
[3]Noble Research Institute, LLC. Ardmore, OK 73401, USA

SUMMARY

Calcineurin is a conserved calcium/calmodulin-dependent protein phosphatase, consisting of a catalytic subunit A and a regulatory subunit B, which is involved in calcium-dependent signalling and regulation of various important cellular processes. In this study, we functionally characterized the catalytic subunit A (CnaA) of the endophytic fungus *Epichloë festucae* which forms a symbiotic association with the grass host *Lolium perenne*. We deleted the CnaA-encoding gene *cnaA* in *E. festucae* and examined its role in hyphal growth, cell wall integrity and symbiosis. This Δ*cnaA* strain had a severe growth defect with loss of radial growth and hyper-branched hyphae. Transmission electron microscopy and confocal microscopy analysis of the mutant revealed cell wall defects, aberrant septation and the formation of intrahyphal hyphae, both in culture and *in planta*. The mutant strain also showed a reduced infection rate *in planta*. The fluorescence of mutant hyphae stained with WGA-AF488 was reduced, indicating reduced chitin accessibility. Together, these results show that *E. festucae* CnaA is required for fungal growth, maintaining cell wall integrity and host colonization.

Keywords: calcineurin, CnaA, *Epichloë*, hyphal growth.

INTRODUCTION

Calcineurin is a eukaryote calcium/calmodulin-dependent serine/threonine-specific protein phosphatase, and one of the best-characterized components of calcium signalling pathways. This enzyme is a heterodimer containing catalytic subunit calcineurin A (CnaA) and regulatory subunit calcineurin B (CnaB). Calmodulin binds to the calcineurin AB heterodimer in response to increased cytosolic calcium levels, releasing the CnaA autoinhibitory domain, thereby activating phosphatase activity, which, in turn, dephosphorylates downstream target proteins (Rumi-Masante *et al.*, 2012; Rusnak and Mertz, 2000). In fungi, calcineurin signalling is mediated through the calcineurin-responsive transcription factor CRZ1, which plays a crucial role in the regulation of expression of genes involved in controlling ion stress, cell wall integrity, hyphal growth and a number of other developmental processes (Stie and Fox, 2008; Thewes, 2014). Calcineurin has been widely studied in human fungal pathogens, where it has been shown to regulate events essential for pathogenesis, such as the growth of *Cryptococcus neoformans* at 37 °C (Cruz *et al.*, 2001). In *Candida albicans*, calcineurin is involved in multi-drug resistance (Hameed *et al.*, 2011) and the maintenance of cell wall integrity through the regulation of the chitin synthesis genes *chs2* and *chs8* (Munro *et al.*, 2007). Studies in *Aspergillus fumigatus* have demonstrated a crucial role for calcineurin in hyphal elongation and septa formation (Juvvadi *et al.*, 2011, 2016; da Silva Ferreira *et al.*, 2007).

Calcineurin signalling has also been investigated in fungal–plant associations. In *Ustilago maydis*, the causative agent of corn smut disease, calcineurin is essential for virulence, with mutants unable to form tumours on infected plants (Egan *et al.*, 2009). In *Ustilago hordei*, which causes barley smut disease, the deletion of both calcineurin subunit genes results in decreased host infection rates (Cervantes-Chavez *et al.*, 2011). In *Magnaporthe oryzae*, appressorium formation is blocked when cultures are treated with the calcineurin inhibitor cyclosporin A or when the calcineurin A gene, *MCNA*, is silenced by RNAi (Choi *et al.*, 2009b). Disruption of *M. oryzae CRZ1* confirmed that calcineurin signalling is required for the infection process, with mutants seldom developing infectious hyphae (Choi *et al.*, 2009a), possibly as a result of the reduced turgor pressure of the mutant (Zhang *et al.*, 2009). *Botrytis cinerea crz1* mutants are defective in host penetration, but this phenotype can be rescued by osmotic stabilizers, demonstrating the importance of cell wall integrity for host colonization by fungal pathogens (Schumacher *et al.*, 2008). Although these examples highlight the importance of calcineurin for host colonization, the precise role of this protein in each of these processes is not yet fully understood.

The endophytic fungus *Epichloë festucae* forms a highly regulated mutualistic interaction with perennial ryegrass (*Lolium perenne*). In this association, fungal hyphae grow in the intercellular

*Correspondence: Email: d.b.scott@massey.ac.nz

spaces of the host plant, a biological niche that provides a source of nutrients, a stable environment and a transmission vector through host seeds (Schardl *et al*., 2004). Perennial ryegrass plants infected with *E. festucae* show enhanced tolerance to various biotic and abiotic stresses, including protection from insect herbivory (Tanaka *et al*., 2005) and enhanced drought tolerance (Hahn *et al*., 2008). Studies have shown that the association between *E. festucae* and *L. perenne* represents a good model system for the study of mutualistic fungal–grass interactions, particularly the signalling pathways required for the maintenance of a stable interaction (Scott, 2001). Disruption of NADPH oxidase-catalysed reactive oxygen species (ROS) production in the fungus leads to a dramatic breakdown in fungal–host signalling characterized by a switch from restrictive to proliferative fungal growth, the loss of host apical dominance and premature host senescence (Takemoto *et al*., 2006; Tanaka *et al*., 2006, 2008). The deletion of two *E. festucae* genes encoding mitogen-activated protein (MAP) kinases, *sakA* (stress-activated) and *mpkA* (cell wall integrity, CWI), also impacts severely on the association, resulting in major effects on host growth and development similar to those observed for pathogenic interactions (Becker *et al*., 2015; Eaton *et al*., 2010). High-throughput mRNA sequencing of wild-type (WT) and Δ*sakA* mutant associations revealed dramatic changes in both fungal and plant gene expression, showing that the host recognizes the *sakA* mutant as a pathogen (Eaton *et al*., 2010). These studies clearly demonstrate the importance of fungal signalling pathways in the regulation of the *E. festucae*–perennial ryegrass association.

Given the importance of calcineurin signalling in fungal pathogenesis, we set out to determine the role of this pathway in the mutualistic symbiotic interaction between *E. festucae* and its grass host *L. perenne*. A reverse genetic approach was used to functionally characterize the role of the *E. festucae* calcineurin catalytic subunit through studies of Δ*cnaA* mutants in axenic culture and *in planta*.

RESULTS

Some *Epichloë* species contain multiple copies of *cnaA*

To determine whether *E. festucae* possesses a gene encoding the calcineurin catalytic subunit CnaA, a tBLASTn search of the *E. festucae* Fl1 and *E. festucae* E2368 genome sequences (Schardl *et al*., 2013) was carried out using *Aspergillus nidulans*, *Neurospora crassa* and *Saccharomyces cerevisiae* CnaA sequences as queries. This search identified one homologue in *E. festucae* Fl1 (*cnaA*; gene model EfM3.035130) and two homologues in *E. festucae* E2368 (*cnaA1* and *cnaA2*; gene models EfM3.035130 and EfM3.051970). The two *cnaA* homologues in *E. festucae* E2368 were located at distinct genomic loci. The *cnaA2* locus was rich in repetitive elements compared with the *cnaA* and *cnaA1* loci (Fig. 1a). The nucleotide sequences of *E. festucae* Fl1 *cnaA* and *E. festucae* E2368 *cnaA1* were identical, with open reading frames (ORFs) of 1692 bp encoding polypeptides of 563 amino acids. The nucleotide sequence of *E. festucae* E2368 *cnaA2* had a 1830-bp ORF encoding a 609-amino-acid polypeptide. The translated amino acid sequences of *E. festucae* CnaA1 and CnaA2 shared 67% identity. The *E. festucae* CnaA1 and CnaA2 sequences were aligned with CnaA sequences from other species, including *A. nidulans*, *N. crassa*, *S. cerevisiae*, *A. fumigatus*, *Fusarium oxysporum* and *Homo sapiens*. This alignment showed that the *E. festucae* homologues contained all conserved domains characteristic of calcineurin catalytic A proteins, namely the catalytic domain, the calcineurin B-binding domain, the calmodulin-binding domain and the autoinhibitory domain (Fig. 1b). This supported the identification of the *E. festucae* CnaA proteins as calcineurin catalytic A subunits. All domains were highly conserved amongst the species analysed (Fig. 1b). A search of the *E. festucae* Fl1 and *E. festucae* E2368 genome sequences for a gene encoding the calcineurin regulatory subunit CnaB identified one homologue (gene model EfM3.027360) in each genome.

A BLASTn search of 17 other sequenced *Epichloë* genomes (Schardl *et al*., 2013) using *cnaA*, *cnaA1* and *cnaA2* as the query sequences identified only one homologue of *cnaA*/*cnaA1* in each genome, except that of *Epichloë uncinata*, which contained two *cnaA*/*cnaA1* homologues (Table S1, see Supporting Information). Given that *E. uncinata* is an interspecific hybrid of *Epichloë bromicola* and *Epichloë typhina* ssp. *poae* (Leuchtmann *et al*., 2014), the two *cnaA*/*cnaA1* copies probably derive from these parental strains. No *cnaA2* homologues were identified. Using Southern analysis, we further analysed 20 other *Epichloë* strains whose genomes have not been sequenced for duplication of *cnaA*. This analysis identified three *E. festucae* strains (*E. festucae* E189, *E. festucae* Fr1 and *E. festucae* 1035.33) and three strains from other *Epichloë* species (*Epichloë elymi* WWG1, *E. elymi* WWG3 and *Epichloë baconii* E424) which appeared to contain *cnaA2* (Fig. S1, see Supporting Information). However, *E. festucae* strain E189 is the parent of both E2368 and E1035.33.

Deletion of *E. festucae* Fl1 *cnaA* causes severe growth defects in culture

To study the role of calcineurin signalling in *E. festucae* hyphal growth and the interaction of this endophyte with its host *L. perenne*, we generated an *E. festucae* Fl1 *cnaA* deletion strain by transforming protoplasts of *E. festucae* Fl1 with a restriction enzyme-generated fragment from pMMI4 containing a hygromycin resistance gene (see Experimental procedures). Polymerase chain reaction (PCR) screening of hygromycin-resistant (Hyg^R) transformants identified two strains (Δ*cnaA*#12 and Δ*cnaA*#27) with banding patterns characteristic of targeted replacement events. Southern analysis of genomic DNA digests from these transformants confirmed that Δ*cnaA*#12 contained a single

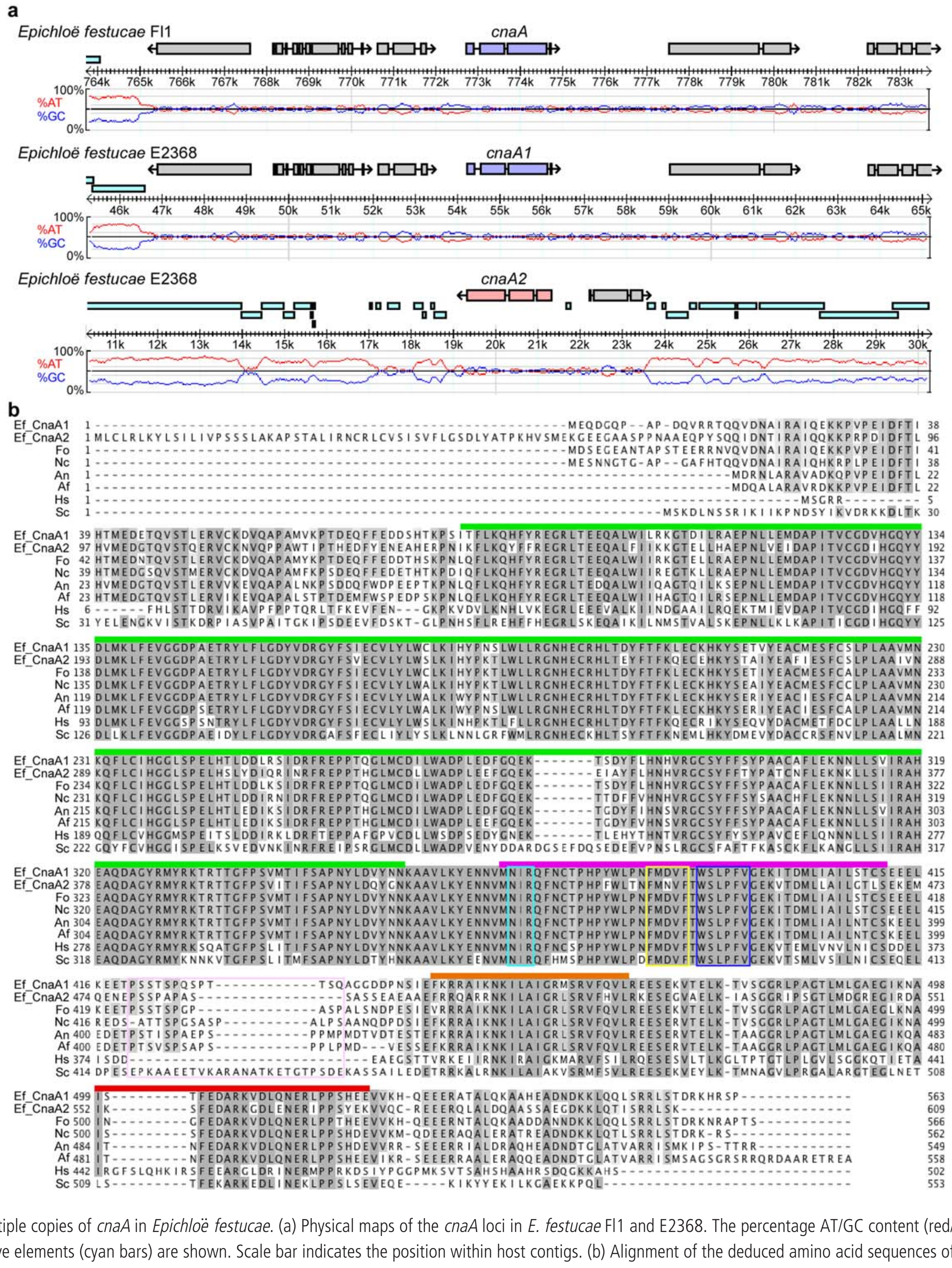

Fig. 1 Multiple copies of *cnaA* in *Epichloë festucae*. (a) Physical maps of the *cnaA* loci in *E. festucae* Fl1 and E2368. The percentage AT/GC content (red/blue traces) and repetitive elements (cyan bars) are shown. Scale bar indicates the position within host contigs. (b) Alignment of the deduced amino acid sequences of *cnaA1* and *cnaA2* from *E. festucae* and *cnaA* from *Fusarium oxysporum* (Fo, XP018243626), *Neurospora crassa* (Nc, XP011394598), *Aspergillus nidulans* (An, P48457), *Aspergillus fumigatus* (Af, XP753703), *Saccharomyces cerevisiae* (Sc, NP013537) and human (Hs, AAB23769). Conserved domains are shown with coloured bars: catalytic (green), calcineurin B-binding (purple), calmodulin-binding (orange) and autoinhibitory region (red).

insertion of the replacement cassette into the *cnaA* locus (Fig. S2, see Supporting Information). This *cnaA* deletion strain (henceforth Δ*cnaA*) was selected for further experiments.

The culture growth phenotype of Δ*cnaA* on potato dextrose agar (PDA) plates was defective compared with WT. The radial growth of Δ*cnaA* was severely reduced and lacked aerial hyphae,

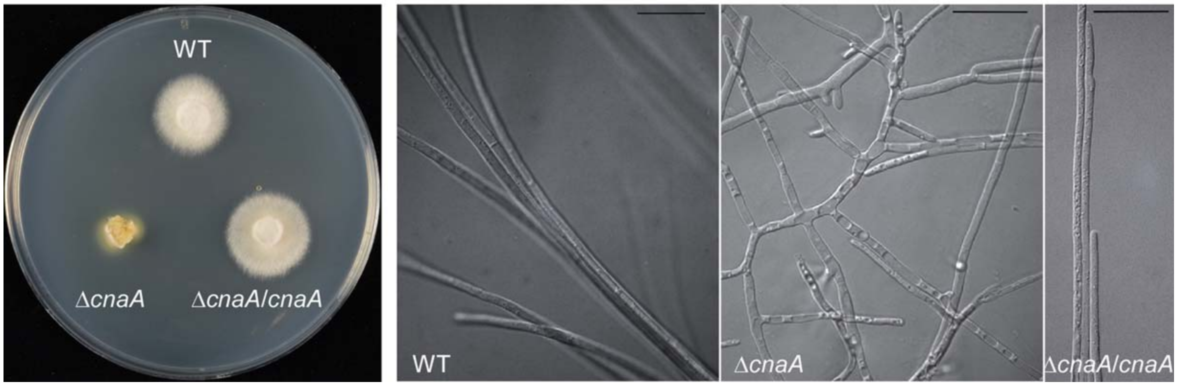

Fig. 2 Deletion of *Epichloë festucae* Fl1 *cnaA* causes severe growth defects in culture. (a) Colony morphology of *E. festucae* Fl1 wild-type (WT), *cnaA* deletion strain (Δ*cnaA*) and Δ*cnaA* strain complemented with WT copy of *E. festucae* Fl1 *cnaA* (Δ*cnaA*/*cnaA*) grown on potato dextrose agar for 6 days. (b) Comparison of differential interference contrast image of Δ*cnaA* culture showing highly deregulated growth pattern with increased branching and altered hyphal morphology compared with the wild-type (WT) and complementation strain (Δ*cnaA*/*cnaA*). Bar, 20 μm.

resulting in a compact colony (Fig. 2a). In addition, a yellow pigment was observed around the periphery of the Δ*cnaA* mycelia which was not observed for WT (Fig. 2a). Differential interference contrast (DIC) microscopic analysis revealed that the Δ*cnaA* strain showed increased and irregularly branched hyphae that were swollen and convoluted (Fig. 2b). Hyphal debris was observed within the area of yellow pigment around the colony. All abnormal phenotypes were fully rescued when WT *cnaA* was reintroduced into the Δ*cnaA* mutant strain (Figs 2,b and S2). Given that Mg^{2+} restores growth defects of calcineurin mutants (Schumacher *et al*., 2008), we investigated the growth of Δ*cnaA* on PDA supplemented with $MgCl_2$. In the presence of Mg^{2+}, growth defects of Δ*cnaA* were partially remediated with increased radial growth and more aerial hyphae, and the lack of a yellow pigment in the medium (Fig. S3, see Supporting Information). Surprisingly, remediation of this phenotype was also observed when compact and dense mycelia of Δ*cnaA* colonies were coarsely ground and spread over PDA (Fig. S3). On account of these observations, we used both non-remediated Δ*cnaA* (henceforth Δ*cnaA* NR) and remediated Δ*cnaA* (henceforth Δ*cnaA* R) colonies for *in planta* experiments (described below).

Epichloë festucae CnaA contributes to cell wall organization

Given that the calcineurin signalling pathway contributes to the regulation of cell wall biosynthesis (Fortwendel *et al*., 2009), we investigated the role of *E. festucae* Fl1 CnaA in chitin synthesis. We specifically tested the Δ*cnaA* mutant strain for chitin distribution in the cell wall by calcofluor white staining. The WT strain showed a distinctive pattern of strongly stained hyphal tips and septa, whereas the Δ*cnaA* mutant strain exhibited an altered staining pattern (Fig. 3). The mutant strain showed a reduced zone of staining at the hyphal tips and a scattered localization of stained aggregations along the apical hyphal compartment (Fig. 3). The mutant strain also exhibited weakly stained irregular septa with shorter hyphal compartments compared with the WT strain, but hyphal anastomosis was not affected. The reintroduction of WT *cnaA* into Δ*cnaA* restored the WT calcofluor white staining pattern (Fig. 3).

As the calcineurin mutant strain showed a defective distribution of cell wall components, we performed transmission electron microscopy (TEM) to examine cell wall organization in the mutant strain grown on PDA plates. This analysis revealed peculiar formations within the calcineurin mutant hyphae that resembled sections of cytoplasm surrounded by a secondary cell wall in the parent cell (Fig. 4a; indicated by yellow arrowheads). In transverse sections, mutant hyphae appeared to have two or three closely packed layers of cell wall (Fig. 4a; lower panel). In addition, the mutant hyphae showed disrupted outer cell walls and incomplete septa (Fig. 4a, lower panel; indicated by red and white arrowheads). This hypha within hypha morphology strongly resembles the phenomenon of intrahyphal hyphae, which is described in filamentous fungi (Becker *et al*., 2015; Calonge, 1968). This phenomenon was studied in detail in *Sclerotinia fructigena* (Calonge, 1968) and drawings produced in that study showed structures very similar to those seen in the Δ*cnaA* strain (Fig. 4b). Together, these results suggest that the deletion of *cnaA* in *E. festucae* Fl1 leads to the disruption of cell wall organization, abnormal septation and the formation of intrahyphal hyphae.

The duplicate *cnaA* genes in *E. festucae* E2368 are functionally redundant

We constructed targeted deletions of *cnaA1* and *cnaA2* to functionally characterize these duplicate genes in *E. festucae* E2368.

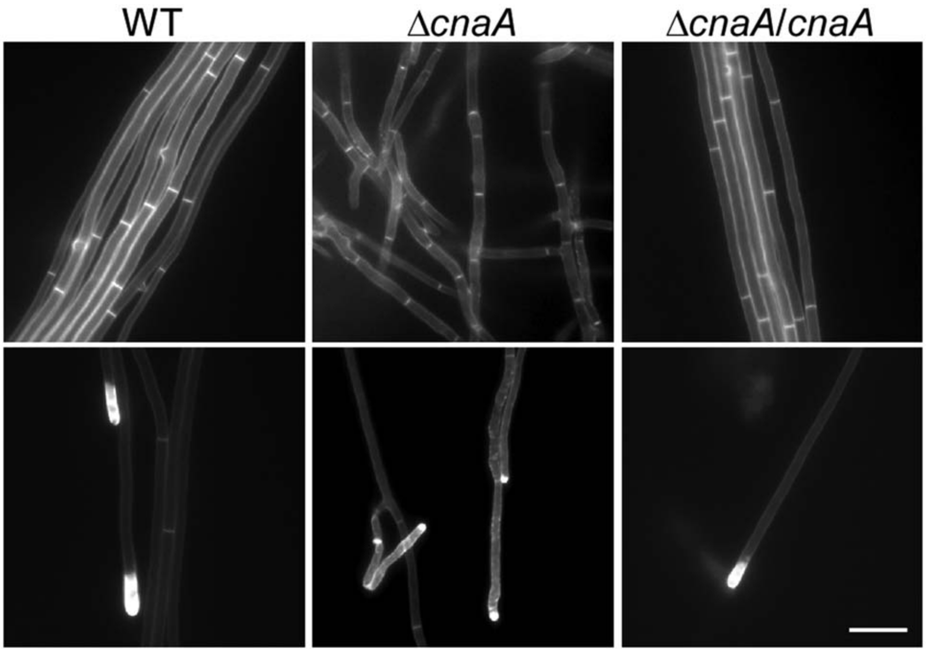

Fig. 3 Deletion of *Epichloë festucae* Fl1 *cnaA* causes defects in septation and the distribution of cell wall components. Confocal images of *E. festucae* Fl1 wild-type (WT), Δ*cnaA* and Δ*cnaA*/*cnaA* cultures stained with calcofluor white, which binds to chitin, showing a loss of the WT staining pattern in the Δ*cnaA* strain. Bar, 20 μm.

Restriction enzyme-generated fragments from pMMI4 and pMMI13, containing replacement cassettes for *cnaA1* and *cnaA2*, respectively, were transformed into *E. festucae* E2368 protoplasts and the resulting transformants were screened for true replacements (Fig. S4, see Supporting Information). This screening identified two deletion strains (Δ*cnaA1*#10 and Δ*cnaA1*#17) for *cnaA1* and two deletion strains (Δ*cnaA2*#24 and Δ*cnaA2*#27) for *cnaA2*. The mutant strains Δ*cnaA1*#17 (henceforth Δ*cnaA1*) and Δ*cnaA2*#27 (henceforth Δ*cnaA2*) were used for further experiments.

Deletion of either *cnaA1* or *cnaA2* did not result in the severe growth phenotype observed for *E. festucae* Fl1 Δ*cnaA* (Figs 5a and 2a). Although the colony morphology and growth rate of the Δ*cnaA2* strain were similar to those of *E. festucae* E2368 WT, the Δ*cnaA1* strain had a slightly slower growth rate relative to WT (Fig. 5a). Given that the *E. festucae* Fl1 *cnaA* and *E. festucae* E2368 *cnaA1* nucleotide sequences were identical, we reasoned that the reintroduction of *cnaA1* into Δ*cnaA* was unnecessary, given that *cnaA* complemented the Δ*cnaA* strain. Hence, we only used *E. festucae* E2368 *cnaA2* to attempt complementation of the

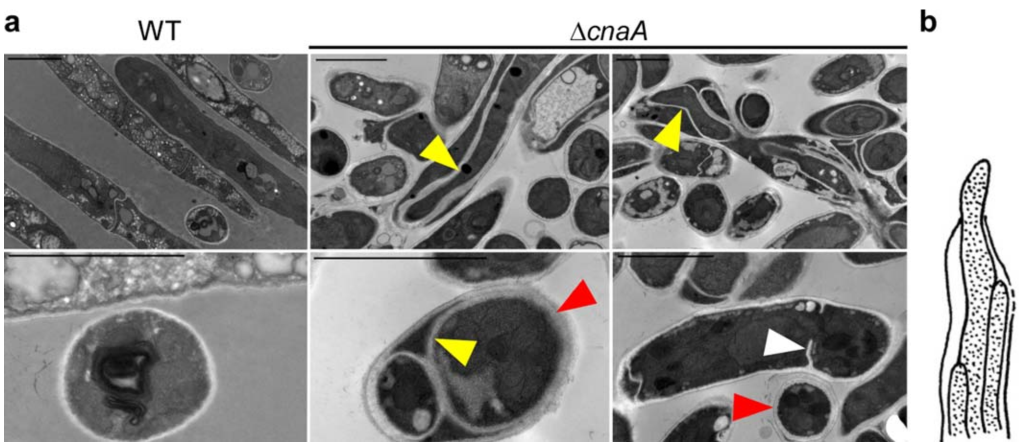

Fig. 4 Deletion of *Epichloë festucae* Fl1 *cnaA* causes the formation of intrahyphal hyphae. (a) Transmission electron micrographs of *E. festucae* Fl1 wild-type (WT) and Δ*cnaA* strains showing extensive formation of intrahyphal cell walls in the mutant hyphae (indicated by yellow arrowheads) and abnormal septa (indicated by white arrowheads). Red arrowheads indicate disrupted outer cell wall. Bar, 2 μm. (b) Reproduction of a drawing from Calonge (1968) showing intrahyphal hyphae breaking out from the mother hypha of *Sclerotinia fructigena*. This schematic diagram captures the transmission electron micrographs of the hyphal structures observed in the Δ*cnaA* strain.

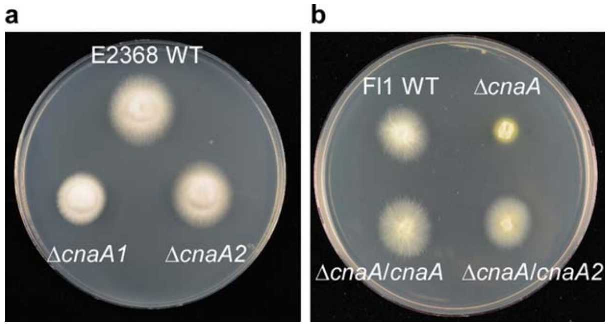

Fig. 5 The duplicate *cnaA* genes of *Epichloë festucae* E2368 are functionally redundant. (a) Colony morphology of *E. festucae* E2368 wild-type (WT), Δ*cnaA1*#17 (Δ*cnaA*1) and Δ*cnaA*2#27 (Δ*cnaA*2) cultures grown on potato dextrose agar for 6 days. (b) Colony morphology of *E. festucae* Fl1 Δ*cnaA* complemented with the WT copy of *E. festucae* E2368 *cnaA2* (Δ*cnaA*/*cnaA2*) grown on potato dextrose agar for 6 days.

E. festucae Fl1 Δ*cnaA* strain. The resulting Δ*cnaA*/*cnaA2* strain restored the growth defects of Δ*cnaA*, indicating that *cnaA1* and *cnaA2* are functionally redundant in culture (Fig. 5b).

Disruption of *cnaA* induces a necrotic response *in planta*

To test the role of calcineurin signalling in the establishment of a symbiotic interaction, *L. perenne* seedlings were inoculated with both non-remediated and remediated Δ*cnaA* strains (Δ*cnaA* NR and Δ*cnaA* R, respectively). Interestingly, seedlings inoculated with Δ*cnaA* NR colonies developed a strong host defence response at 5–9 days post-inoculation that was visible as a brown coloration around the inoculation region (Fig. 6a). The response in some seedlings was strong enough to cause host death. However, a host defence response was absent when seedlings were inoculated with Δ*cnaA* R or WT colonies (Fig. 6a).

Given that inoculum from a Δ*cnaA* NR colony, but not a Δ*cnaA* R colony, caused necrosis of seedling tissue (Fig. 6a), we investigated whether the remediation of mutant colonies induced irreversible changes in the mutant strain. To test this, fungal colonies were grown from tissue of 12-week-old infected plants on PDA plates. Both Δ*cnaA* NR and Δ*cnaA* R colonies showed a similar growth phenotype and grew as compact, dense masses of hyphae, unlike the WT strain (Fig. 6b). This suggests that remediation of mutant colonies does not induce an irreversible change in Δ*cnaA*.

Deletion of *cnaA* in *E. festucae* Fl1 reduces host colonization and induces the formation of intrahyphal hyphae *in planta*

To determine whether CnaA is involved in host colonization, *L. perenne* seedlings were inoculated with *E. festucae* Fl1 WT, Δ*cnaA* (both NR and R colonies) and Δ*cnaA* complementation

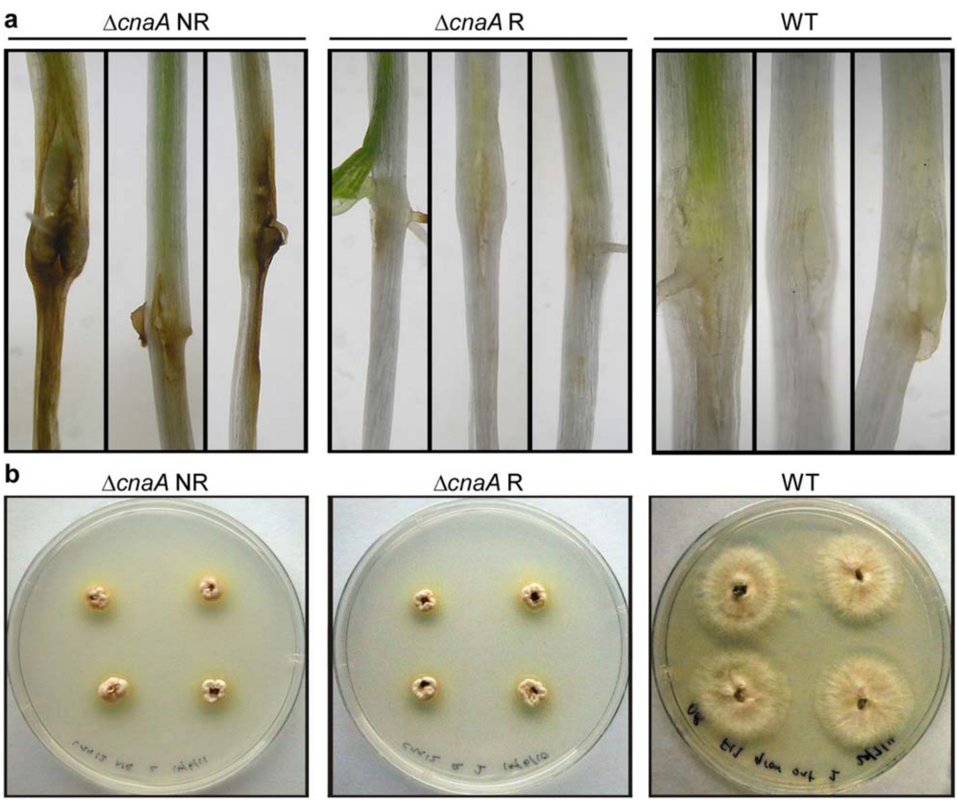

Fig. 6 Deletion of *Epichloë festucae* Fl1 *cnaA* elicits a host defence response in *Lolium perenne* seedlings. (a) Light micrographs of *L. perenne* seedlings at 10 days post-inoculation with non-remediated (Δ*cnaA* NR) and remediated (Δ*cnaA* R) cultures of Fl1 Δ*cnaA* and wild-type (WT). (b) *Epichloë festucae* grow outs from *L. perenne* plants infected with non-remediated Δ*cnaA* (Δ*cnaA* NR), remediated Δ*cnaA* (Δ*cnaA* R) and wild-type (WT) Fl1.

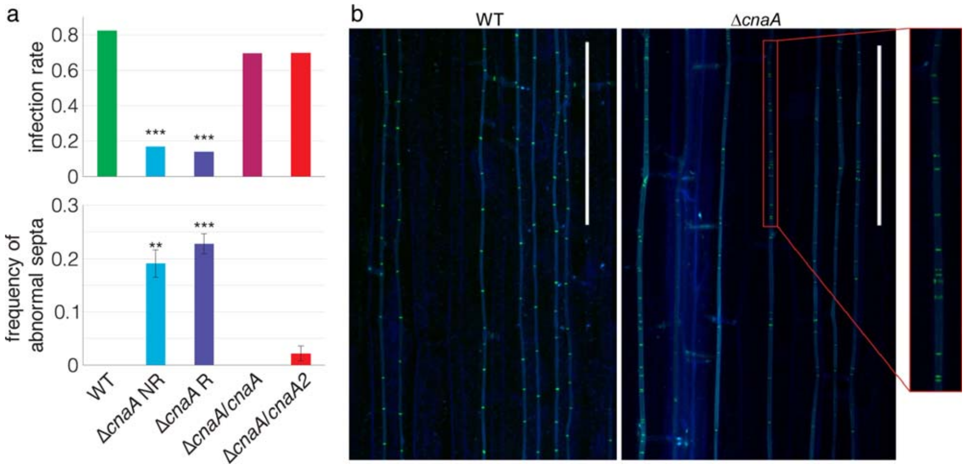

Fig. 7 *Epichloë festucae* Fl1 Δ*cnaA* shows a reduced infection rate and abnormal septal morphology and patterning *in planta*. (a) Deletion of *cnaA* in *E. festucae* reduces the plant infection rate (upper panel). Deletion of *cnaA* in *E. festucae* increases the number of abnormal septa (lower panel). (b) Confocal micrographs of aniline blue- and wheat germ agglutinin-conjugated Alexa Fluor®488 (WGA-AF488)-stained hyphae of wild-type (WT) and Δ*cnaA* mutant *in planta* showing irregular septa formation. Bar, 100 μm.

strains (Δ*cnaA/cnaA* and Δ*cnaA/cnaA2*), and tested for infection at 8 weeks post-inoculation. Both Δ*cnaA* NR and Δ*cnaA* R colonies showed a significantly decreased infection rate *in planta* (Fig. 7a, upper panel). The infection rate *in planta* was restored to WT levels by the introduction of either *cnaA* or *cnaA2* into the Δ*cnaA* strain (Fig. 7a, upper panel). Further, plants infected with Δ*cnaA* NR colonies showed a lower number of hyphae per 100 μm of epidermal peel relative to plants infected with WT. However, the significance of this result was marginal ($t_3 = 3.198$, $P = 0.0498$).

We also investigated the effect of deletion of *cnaA* on septa formation *in planta*. For this analysis, we compared the number of hyphae with abnormal septa between plants infected with WT, Δ*cnaA* and complemented strains. The hyphae from both Δ*cnaA* NR- and Δ*cnaA* R-infected plants showed a significant increase in frequency of abnormal septa (Fig. 7a, lower panel). Although the reintroduction of *cnaA* into Δ*cnaA* completely restored the septal morphology to WT, with no abnormal septa observed in Δ*cnaA/cnaA*, the introduction of *cnaA2* into Δ*cnaA* only partially restored the septal morphology, as abnormal septa were observed for Δ*cnaA/cnaA2*.

We further investigated septa formation *in planta* by confocal microscopy with aniline blue and wheat germ agglutinin-conjugated Alexa Fluor®488 (WGA-AF488) stains, which target β-glucan (blue pseudocolour) and chitin (green pseudocolour), respectively. The WT hyphae showed characteristic blue-stained hyphal cell walls with evenly spaced bright green septa (Fig. 7b). In contrast, septa in Δ*cnaA* were not evenly distributed and were also not as brightly stained as in WT hyphae (Fig. 7b). Hyphae in Δ*cnaA* contained regions in which multiple septa were formed in very close proximity, suggesting defects in hyphal compartmentalization. Although Δ*cnaA* hyphae were defective in septum formation, the parallel restrictive growth of Δ*cnaA* hyphae *in planta* was similar to that of WT. We further investigated the disruption in the formation of hyphal compartments using light microscopy and TEM. The epidermal peels of infected plants were stained with aniline blue and analysed by light microscopy. This analysis revealed a distinctive constricted pattern in Δ*cnaA* hyphae (Fig. 8a). As with the structures seen in cultures grown on PDA plates, this pattern resembled the intrahyphal hyphae structures described previously in *S. fructigena* (Fig. 8b) (Calonge, 1968). The presence of intrahyphal hyphae *in planta* was confirmed using TEM. In transverse sections, Δ*cnaA* hyphae showed multiple cell wall layers within a single hypha (Fig. 8c; indicated by white arrowheads).

DISCUSSION

Calcineurin plays a very important role in coordinating the cellular responses to Ca^{2+} signalling from lower eukaryotes to humans, and is essential for pathogenic fungal adaptation to environmental stress, survival, virulence and pathogenicity. It also regulates hyphal growth, cell wall integrity, appressoria development and mating in other fungi. In this study, we investigated the function of the calcineurin catalytic subunit A (*cnaA*) in the endophytic fungus *E. festucae*, a mutualistic symbiont of grasses. We generated *E. festucae cnaA* deletion strains and showed that this gene is very important for fungal growth and in the colonization of the grass host *L. perenne*.

Calcineurin is a highly conserved protein and consists of two subunits: the catalytic subunit A (CnaA) and the regulatory subunit B (CnaB). Although the genomes of most fungi contain a single *cnaA* copy, we found two *cnaA* paralogues in *E. festucae* E2368 and several other *Epichloë* strains. The presence of multiple *cnaA*

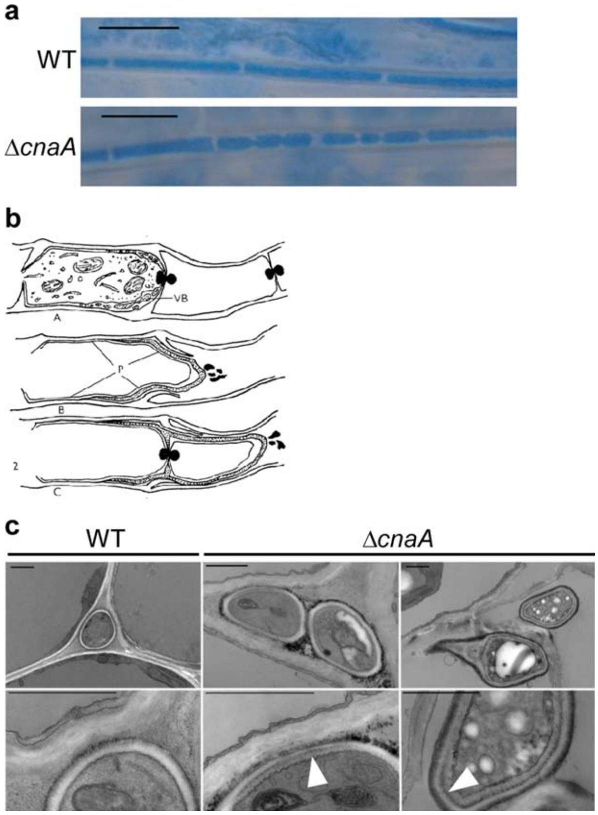

Fig. 8 Deletion of *cnaA* in *Epichloë festucae* Fl1 causes the formation of intrahyphal hyphae *in planta*. (a) Light micrographs of aniline blue-stained hyphae of Δ*cnaA* and wild-type (WT) showing constricted hyphae and increased septa formation in Δ*cnaA* relative to WT. Bar, 10 μm. (b) Reproduction of a drawing from Calonge (1968) showing intrahyphal hyphae breaking out from the mother hypha of *Sclerotinia fructigena*. This schematic diagram captures the light micrograph image of the hyphal structures observed *in planta* for *E. festucae* Δ*cnaA* hyphae. (c) Transmission electron micrographs of wild-type (WT) and Δ*cnaA* mutant *in planta* showing duplication of the cell wall in mutant hyphae, suggesting the presence of intrahyphal hyphae. White arrowheads point to a double cell wall. Bar, 1 μm.

copies has also been reported for fungi of the Clavicipitaceae family, *Beauveria bassiana* and *Cordyceps militaris*, which contain two paralogues each (Li *et al*., 2015), whereas the genomes of fungi in the Zygomycetes family, *Mucor circinelloides* and *Rhizopus delemar*, contain three paralogues each (Lee *et al*., 2013). These *cnaA* genes are often flanked with the same repetitive sequences, which might explain the occurrence of multiple *cnaA* genes through individual gene duplication events (Lee *et al*., 2013).

Calcineurin has both general and specific roles in different organisms. In some fungi, the calcineurin catalytic subunit is an essential gene, including in *A. nidulans*, where it plays a role in growth arrest at an early stage of the cell cycle (Alshahni *et al*., 2016; Prokisch *et al*., 1997; Rasmussen *et al*., 1994; Viaud *et al*., 2003). However, in most fungi, the deletion or knockdown of the calcineurin catalytic subunit results in defective hyphal morphology. Such strains with an impaired calcineurin signalling pathway show severely restricted growth phenotypes, with compact colonies and highly branched and stunted hyphae (Choi *et al*., 2009b; Egan *et al*., 2009; Harren *et al*., 2012; Odom *et al*., 1997; Steinbach *et al*., 2006). Although *E. festucae cnaA* is not an essential gene, the deletion of *cnaA* caused a severe growth defect in *E. festucae*. The mutant strain showed markedly reduced radial growth, with irregular, highly branched hyphae and loss of aerial hyphae. In addition, the Δ*cnaA* mutant showed abnormal septation, with unevenly distributed and irregularly spaced septa that were often in close proximity, resulting in high variability in hyphal compartment length. These phenotypes are similar to the Δ*cnaA* mutant phenotypes of *B. cinerea* and *A. fumigatus* (Harren *et al*., 2012; Juvvadi *et al*., 2011). Interestingly, although individual *A. fumigatus* Δ*cnaA* and Δ*cnaB* strains showed abnormal septa that were curved and wavy, incomplete septation was only observed in *A. fumigatus* Δ*cnaA*/Δ*cnaB* double-deletion strains (Juvvadi *et al*., 2011). In contrast, we observed incomplete septation in the single-deletion Δ*cnaA* strain. Abnormal septation was also observed for chitin synthase deletion strains in *A. nidulans* and *A. fumigatus* (Fukuda *et al*., 2009; Ichinomiya *et al*., 2005; Muszkieta *et al*., 2014). These defective hyphal morphology and abnormal septation features of Δ*cnaA* mutants indicate changes in cell wall composition. In filamentous fungi, chitin is a major component of the cell wall that is progressively deposited at the hyphal tips and septa during hyphal growth. In our Δ*cnaA* mutant strain, we observed disrupted distribution of chitin along the hyphae. In other fungi, a link between remodelling of chitin and glucan cell wall components and the calcineurin signalling pathway has been shown. For example, in *A. fumigatus*, calcineurin has been shown to control β-glucan and chitin levels through the down-regulation of β-1,3-glucan synthase catalytic subunit and chitin synthase-encoding genes (Cramer *et al*., 2008; Fortwendel *et al*., 2009; Juvvadi *et al*., 2011). Similar down-regulation of glucan synthase-encoding genes as a result of calcineurin pathway impairment has also been observed in *M. oryzae*, *C. albicans* and *Beauveria bassiana* (Choi *et al*., 2009a; Li *et al*., 2015; Sanglard *et al*., 2003). In contrast, the expression of *U. hordei* and *C. neoformans* glucan synthase-encoding genes was increased in a calcineurin-dependent manner (Cervantes-Chavez *et al*., 2011; Kraus *et al*., 2003). These observations suggest that components of the calcineurin pathway act via distinct mechanisms for the remodelling of cell wall components in ascomycetes versus basidiomycetes. Interactions between the components of protein kinase C, high-osmolarity glycerol (HOG) and calcineurin pathways have been observed to regulate chitin and glucan synthesis (Cervantes-Chavez *et al*., 2011; Juvvadi and Steinbach, 2015; Munro *et al*., 2007). Interestingly, calcineurin also interacts with the components of the HOG pathway to regulate the synthesis of secondary metabolites, as shown in *Arthroderma vanbreuseghemii*, where calcineurin A affects the production of a yellow pigment under hyperosmotic conditions (Alshahni *et al.*, 2016). In our study, the Δ*cnaA* strain secreted a yellow pigment into the agar medium that was not observed for the WT strain. Yellow pigment production, together with the hyphal growth defects observed in the mutant strain, were remediated in the presence of osmotic stabilizers.

The localization of calcineurin subunits at the hyphal tip and septum, and calcineurin complex activity at the hyphal septum, is essential for normal hyphal elongation and proper septation (Juvvadi *et al.*, 2011). Various domains in calcineurin have been implicated for localization and function at the septum. The FMDVF motif that forms a bridge between two known substrate-binding motifs, PxIxIT and LxVP, is required for septal localization and calcineurin function (Juvvadi *et al.*, 2016). *Epichloë festucae* CnaA also possesses this motif, together with the serine–proline-rich region (SPRR) proposed to be important for hyphal growth and virulence through phosphorylation of the SPRR domain (Juvvadi *et al.*, 2013).

In addition to aberrant hyphal morphology and septation, the Δ*cnaA* strain also formed intrahyphal hyphae, both in culture and *in planta*. The formation of intrahyphal hyphae is widespread in fungi, occurring in response to hyphal and/or cellular damage (Bowman *et al.*, 2006; Calonge, 1968; Takeshita *et al.*, 2006). Such structures have been observed previously in CWI MAP kinase, membrane-associated protein and component of striatin-interacting phosphatase and kinase complex mutants of *E. festucae*; chitin synthase mutants of *A. nidulans*, *Fusarium graminearum* and *Colletotrichum graminicola*; and glycosylphosphatidylinositol synthesis gene mutants of *N. crassa* and *C. graminicola* (Becker *et al.*, 2015; Bowman *et al.*, 2006; Green *et al.*, 2016, 2017; Horiuchi *et al.*, 1999; Kim *et al.*, 2009; Oliveira-Garcia and Deising, 2016; Werner *et al.*, 2007). In *A. fumigatus*, intrahyphal hyphae formation was promoted by treatment with caspofungin, which inhibits β-1,3-glucan synthase (Walker *et al.*, 2015). These observations suggest that the formation of intrahyphal hyphae derives from defects in CWI, and it has been proposed to promote fungal survival under stress conditions (Kim and Hyun, 2007). Although the mechanisms governing the formation of intrahyphal hyphae are not clear, Woronin body sealing of septal pores has been proposed to play an important role (Becker *et al.*, 2016).

Calcineurin is also required for virulence and pathogenesis in diverse pathogenic fungi, including *C. neoformans*, *C. albicans*, *A. fumigatus*, *Sclerotinia sclerotiorum*, *M. oryzae*, *U. maydis*, *U. hordei* and *B. cinerea*, but acts through distinct molecular mechanisms (Blankenship *et al.*, 2003; Cervantes-Chavez *et al.*, 2011; Choi *et al.*, 2009b; Cruz *et al.*, 2001; Egan *et al.*, 2009; Harel *et al.*, 2006; Odom *et al.*, 1997; Schumacher *et al.*, 2008; da Silva Ferreira *et al.*, 2007; Steinbach *et al.*, 2006). Although *E. festucae* forms a symbiotic interaction with *L. perenne*, the NADPH oxidase *nox* mutants have been shown to cause a defence response in ryegrass plants, inducing cell wall thickening and increased callose deposition (Becker *et al.*, 2016). Inoculation of *L. perenne* seedlings with Δ*cnaA* induced a necrosis response. One hypothesis is that the yellow pigment produced by Δ*cnaA* NR acts as an elicitor. This hypothesis is supported by observations that the Δ*cnaA* R strain, which did not produce the yellow pigment and was similar to the WT strain in terms of hyphal morphology, failed to induce a necrosis response. However, it remains to be investigated whether this yellow pigment is also produced by the mutant strain *in planta*. The hyphal morphology of Δ*cnaA* *in planta* was comparable with that in culture, except for the lack of hyper-branching, with defects in cell wall organization, abnormal septation and intrahyphal hyphae formation. The Δ*cnaA* strain showed significantly reduced host colonization. In filamentous plant-pathogenic fungi, the calcineurin pathway has been shown to be important for virulence by affecting infection-related morphogenesis (Choi *et al.*, 2009b; Egan *et al.*, 2009). In *B. cinerea*, defects in the calcineurin pathway result in defective mycelium-derived infection (Schumacher *et al.*, 2008). This is improved by Mg^{2+} supplementation, suggesting that cell wall stability contributes to infection and subsequent hyphal growth. Although *E. festucae* forms expressoria (appressorium-like structures that allow endophytic hyphae to exit the host through the cuticle), appressoria-like structures that allow entry to the host have not been observed (Becker *et al.*, 2016). Based on these observations and our study, we suggest that the reduced colonization of plants by the Δ*cnaA* strain is caused by defects in cell wall stability.

In summary, we have identified and functionally characterized the calcineurin catalytic subunit A gene (*cnaA*) in *E. festucae*. We have shown that *E. festucae cnaA* plays an important role in hyphal growth, cell wall organization and intrahyphal hyphae formation, both in culture and *in planta*. Calcineurin A also plays a significant role in the colonization of the host plant.

EXPERIMENTAL PROCEDURES

Strains and growth conditions

Escherichia coli cultures were routinely grown in lysogeny broth (LB) or on LB agar containing ampicillin (100 μg/mL), as described previously (Miller, 1972).

Epichloë festucae cultures were routinely grown on 2.4% PDA or in potato dextrose broth (PDB), as described previously (Moon *et al.*, 1999, 2000). For genomic DNA extraction for PCR screening, *E. festucae* cultures were grown from mycelia (approximately 1-cm^2 section) in 150 μL of 2.4% PDB for 3 days. A description of all biological materials used in this study is given in Table S2 (see Supporting Information).

Plant growth and endophyte inoculation conditions

Endophyte-free seedlings of perennial ryegrass *L. perenne* cv. Samson were inoculated with *E. festucae*, as described previously (Latch and Christensen, 1985). Plants were grown in root trainers in an environmentally controlled growth room at 22 °C with a photoperiod of 16 h light (approximately 100 μE/m^2/s). At 8 weeks post-inoculation, plants were tested for endophyte infection by immunoblotting (Tanaka *et al.*, 2005).

DNA extraction, PCR and sequencing

Plasmid DNA was extracted using a High Pure Plasmid Isolation Kit (Roche, Basel, Switzerland) according to the manufacturer's instructions. Fungal genomic DNA for PCR screening to identify gene replacement mutants was extracted from mycelia. These mycelia were grown in 150 μL of 2.4% PDB, collected by centrifugation and ground in 150 μL of lysis buffer [100 mM tris(hydroxymethyl)aminomethane (Tris), 100 mM sodium ethylenediaminetetraacetate (Na_2-EDTA), 1% sodium dodecylsulfate (SDS), pH 8.0]. The mixture was incubated at 70 °C for 30 min, followed by the addition of 150 μL of 5 M potassium acetate and a further 10 min of incubation on ice. Samples were then centrifuged at 17,000 g for 10 min. The supernatant was transferred into a fresh Eppendorf tube and 0.6 vol of isopropanol was added. DNA was pelleted by centrifugation at 17,000 g for 15 min. The pelleted DNA was washed in 70% ethanol, air dried and resuspended in 20 μL of sterile milli-Q water. A 2-μL sample was used as template for PCR. Fungal genomic DNA for Southern analysis and for the generation of fragments used in plasmid construction was extracted from freeze-dried mycelia, as described previously (Byrd *et al.*, 1990).

Standard PCR and PCR screening were performed with *Taq* DNA polymerase (Roche) according to the manufacturer's instructions in a 50-μL reaction volume. When proofreading activity was required, PCR was performed with *Pfx*50^{TM} DNA polymerase (Invitrogen, Carlsbad, CA, USA) according to the manufacturer's instructions.

DNA fragments were sequenced using the dideoxynucleotide chain termination method with the Big-Dye Terminator Version 3.1 Ready Reaction Cycle Sequencing Kit (Applied BioSystems, Carlsbad, CA, USA) and separated using an ABI3730 genetic analyser (Applied BioSystems, MacVector Inc., Apex, NC, USA). Sequence data were assembled and analysed using MacVector sequence assembly software, version 12.0.5.

Preparation of deletion and complementation constructs

The lists of all plasmids and primers used in the preparation of the constructs are given in Tables S2 and S3 (see Supporting Information).

The *E. festucae* Fl1 *cnaA* and *E. festucae* E2368 *cnaA1* replacement construct pMMI4 was generated by cloning restriction enzyme-digested fragments from *E. festucae* Fl1 cosmid 2C5. This cosmid was isolated from an *E. festucae* Fl1 cosmid library (Tanaka *et al.*, 2005) by colony hybridization using a probe specific for Fl1 *cnaA*, which was amplified with primers MI13 and MI14 using *E. festucae* Fl1 genomic DNA as template. A 1.4-kb *Pst*I/*Bam*HI fragment 5′ of *cnaA* was cloned 3′ of the *hph* cassette and a 2.1-kb *Eco*RI/*Eco*RV fragment 3′ of *cnaA* was cloned 5′ of the *hph* cassette in the plasmid pSF15.15, generating the *cnaA*/*cnaA1* replacement construct pMMI4. The *E. festucae* E2368 *cnaA2* replacement construct pMMI13 was generated using PCR-amplified fragments. A 1.95-kb PCR fragment 5′ of *cnaA2* was amplified with primers 1372-2F and cna1372R and cloned into the vector pCR4-TOPO. From the resultant plasmid, a 1.7-kb *Eco*RI fragment containing the 5′ *cnaA2* flanking sequence was obtained and cloned into plasmid pSF17.8. A 1.28-kb PCR fragment 3′ of *cnaA2* was amplified with primers cna2F and 1372-5R, and cloned into the vector pCR4-TOPO. From the resultant plasmid, a 1.5-kb *Eco*RI fragment containing the 3′ *cnaA2* flanking sequence was obtained and cloned into plasmid pSF13.5. From this plasmid, a 1.5-kb *Xba*I fragment containing the 3′ *cnaA2* flanking sequence was obtained and cloned into plasmid pSF17.8 containing the 5′ *cnaA2* flanking sequence, giving the *cnaA2* replacement construct pMMI13. The *cnaA* complementation construct pMMI11 was prepared by cloning a 6-kb *Eco*RV fragment from cosmid 2C5 into plasmid pSF17.8. The *cnaA2* complementation construct pMMI12 was prepared by cloning a 4.5-kb PCR fragment amplified with primers 1372-2F and 1372-5R into the vector pII99.

Epichloë festucae transformation and screening for mutants

Epichloë festucae protoplasts were prepared as described previously (Young *et al.*, 2005). However, because of its slow growth, mycelia for the preparation of *E. festucae* Fl1 Δ*cnaA* protoplasts were grown for 10 days instead of 7 days. Protoplasts were transformed with 5 μg of linear PCR-amplified, restriction enzyme-digested or circular plasmid DNA using the method described previously (Itoh *et al.*, 1994). Transformants were selected on regeneration medium (PDA medium supplemented with 0.8 M sucrose) containing either hygromycin (150 μg/mL) or geneticin (200 μg/mL), and nuclear-purified by three rounds of subculture on selection medium.

To generate *E. festucae* Fl1 *cnaA* and *E. festucae* E2368 *cnaA1* deletion strains, protoplasts of these strains were transformed with a linear 5-kb *Hin*dIII/*Eco*RV fragment from pMMI4, and transformants were selected on medium containing hygromycin. Transformants were screened with primers MI13 and MI14 to distinguish WT (1-kb) from replacement sequences (no PCR product). To generate *E. festucae* E2368 *cnaA2* deletion strain, E2368 protoplasts were transformed with a linear 5-kb *Xho*I/*Hpa*I fragment from pMMI13, and transformants were selected on medium containing geneticin. Transformants were screened with primers MI15 and MI16 to distinguish WT (1-kb) from replacement sequences (no PCR product). For complementation of the *E. festucae* Fl1 Δ*cnaA* strain, Δ*cnaA* protoplasts were transformed with either pMMI11 (containing *E. festucae* Fl1 *cnaA*) or pMMI12 (containing *E. festucae* E2368 *cnaA2*), and transformants were selected on medium containing geneticin. Reintroduction of *cnaA* or *cnaA2* was confirmed by PCR using primers MI13 and MI14 (for *cnaA*) or MI15 and MI16 (for *cnaA2*).

DNA hybridization

Epichloë festucae genomic DNA digests were separated by agarose gel electrophoresis and transferred to positively charged nylon membranes (Roche). DNA was then fixed to membrane by UV light cross-linking in a Cex-800 UV light cross-linker (Ultra-Lum, Claremont, CA, USA) at 254 nm for 2 min. DNA probes were labelled with [α-^{32}P]-dCTP (3000 Ci/mmol; Amersham Biosciences, Buckinghamshire, UK) using a High Prime DNA labelling kit (Roche), and hybridizations were performed according to the manufacturer's instructions. Hybridized bands were visualized by autoradiography.

Microscopy

Epichloë festucae cultures for examination by microscopy were taken directly from PDA plates by excising a 0.2-cm^2 piece of mycelium from the plate, placed on a microscope slide and covered with a cover slip. Bright field microscopy was performed using a Zeiss (Oberkochen, Germany) Axiophot light microscope and images were recorded using a Leica (Wetzlar, Germany) DCF320 digital camera. Light microscopy was used to examine the growth of 6-day-old *E. festucae* strains in culture by DIC, using a $\times$100 immersion objective. Calcofluor white staining was performed by immersing mycelia in 3 mg/mL calcofluor solution (Sigma, St. Louis, MO, USA), incubation in the dark for 30 min and observation under an Olympus IX71 inverted fluorescence microscope using a $\times$60 immersion objective and the filter setting for the capture of calcofluor white.

Epichloë festucae hyphae *in planta* were visualized by taking epidermal peels from the inner surfaces of the outer leaf sheaths and mounting them in aniline blue stain [88% lactic acid, 50% glycerol, 0.1% (w/v) aniline blue], which stains hyphal cytoplasm. The leaf was immersed in aniline blue stain, covered with a cover slip, heated briefly to aid penetration of the stain and examined by light microscopy using $\times$20 and $\times$100 objectives. Confocal microscopy was performed using a Leica SP5 DM6000B confocal microscope. Confocal microscopy was used to visualize chitin distribution and hyphae and septa in the *in planta* sample employing WGA-AF488 staining (Molecular Probes/Invitrogen, Eugene, OR, USA). For WGA-AF488 staining, infected plant tissue was treated overnight in 95% ethanol at 4 °C, and then with 10% potassium hydroxide for 3 h. Tissue was then washed three times with phosphate buffered saline (PBS) (pH 7.4) and incubated in staining solution (0.2% aniline blue, 0.2% Tween-20, 0.01 mg/mL WGA-AF488 in PBS, pH 7.4). Confocal images were taken using a $\times$40 objective with excitation at 405 nm (aniline blue) and 488 nm (WGA-AF488). Images were taken as a stack of six focal planes with 2-μm *z*-steps, giving a total thickness of 10 μm. TEM was performed using a Philips (Amsterdam, The Netherlands) CM10 transmission electron microscope and images were recorded using an SIS Morada digital camera. Samples for TEM were taken from either 6-day-old cultures or 8-week-old plants. Plant samples were prepared by cutting transversely through the pseudostem. Tissues were then fixed in 3% glutaraldehyde and 2% formaldehyde in 0.1 M phosphate buffer, pH 7.2, for 1 h, and transverse sections were prepared for TEM, as described previously (Spiers and Hopcroft, 1993).

Abnormal hyphal morphology *in planta* was analysed using $\times$100 aniline blue images. Twenty images were taken per plant, four plants per strain, except for Δ*cnaA*/*cnaA* where three plants were used. Images were taken at sequential lateral locations that contained hyphae (relative to the leaf axis) with no overlap. Images were analysed by counting the total number of hyphae and the number of hyphae showing abnormal morphology. Hyphae were considered to be 'abnormal' if they had swollen regions, were not straight or showed irregular septa. The fraction of abnormal hyphae was then calculated for each plant and the results were compared using a two-sided Student's *t*-test.

The number of hyphae *in planta* was analysed using $\times$20 aniline blue images. The entire lateral width and depth of each peel were imaged at a single longitudinal location using $\times$20 bright field images. Imaging through the entire depth of each peel was achieved by taking five images at 6-μm *z*-step distances apart, starting just below the peel and finishing just above the slide, resulting in a total image depth of approximately 24 μm for each peel. The image analysis program Corel (Ottawa, Ontario, Canada) Draw was used to draw and measure a line through the centre of each peel perpendicular to the leaf axis and to count the number of hyphae that crossed this line. By pooling the data from all peels of each plant, the number of hyphae per 100 μm can be generated and compared between different plants and symbioses. Results were compared using a two-sided Student's *t*-test.

Infection rate analysis

The infection rates of WT, mutant and complementation strains were analysed by inoculating 216 *L. perenne* seedlings per strain over a 3-week period. The significance of infection rate differences between strains was analysed using Fisher's exact test (two-tailed). Infection statistics were performed on surviving plants only, but no statistically significant differences in host death frequency were observed between different strains.

Bioinformatics analysis

Epichloë festucae genomic sequences were obtained from the *E. festucae* Genome Projects at the University of Kentucky (Schardl *et al*., 2013), and other gene and protein sequences were obtained from the National Center for Biotechnology Information (NCBI) database (http://www.ncbi.nlm.nih.gov/). Multiple sequence alignments and identity scores were generated by CLUSTAL W in MacVector version 12.0.5 using the default settings.

ACKNOWLEDGEMENTS

The authors thank Matthew Savoian, Jordan Taylor and Niki Murray (Manawatu Microscopy and Imaging Centre, Massey University, Palmerston North, New Zealand), and Arvina Ram (Massey University), for technical assistance.

REFERENCES

Alshahni, M.M., Shimizu, K., Yoshimoto, M., Yamada, T., Nishiyama, Y., Arai, T. and Makimura, K. (2016) Genetic and phenotypic analyses of calcineurin A subunit in *Arthroderma vanbreuseghemii*. *Med. Mycol.* **54**, 207–218.

Becker, M., Becker, Y., Green, K. and Scott, B. (2016) The endophytic symbiont *Epichloë festucae* establishes an epiphyllous net on the surface of *Lolium perenne* leaves by development of an expressorium, an appressorium-like leaf exit structure. *New Phytol.* **211**, 240–254.

Becker, Y., Eaton, C.J., Brasell, E., May, K.J., Becker, M., Hassing, B., Cartwright, G.M., Reinhold, L. and Scott, B. (2015) The fungal cell-wall integrity MAPK cascade is crucial for hyphal network formation and maintenance of restrictive growth of *Epichloë festucae* in symbiosis with *Lolium perenne*. *Mol. Plant–Microbe Interact.* **28**, 69–85.

Blankenship, J.R., Wormley, F.L., Boyce, M.K., Schell, W.A., Filler, S.G., Perfect, J.R. and Heitman, J. (2003) Calcineurin is essential for *Candida albicans* survival in serum and virulence. *Eukaryot. Cell*, **2**, 422–430.

Bowman, S.M., Piwowar, A., Al Dabbous, M., Vierula, J. and Free, S.J. (2006) Mutational analysis of the glycosylphosphatidylinositol (GPI) anchor pathway demonstrates that GPI-anchored proteins are required for cell wall biogenesis and normal hyphal growth in *Neurospora crassa*. *Eukaryot. Cell*, **5**, 587–600.

Byrd, A.D., Schardl, C.L., Songlin, P.J., Mogen, K.L. and Siegel, M.R. (1990) The beta-tubulin gene of *Epichloë typhina* from perennial ryegrass (*Lolium perenne*). *Curr. Genet.* **18**, 347–354.

Calonge, F.D. (1968) Origin and development of intrahyphal hyphae in *Sclerotinia fructigena*. *Mycologia*, **60**, 932–942.

Cervantes-Chavez, J.A., Ali, S. and Bakkeren, G. (2011) Response to environmental stresses, cell-wall integrity, and virulence are orchestrated through the calcineurin pathway in *Ustilago hordei*. *Mol. Plant–Microbe Interact.* **24**, 219–232.

Choi, J., Kim, Y., Kim, S., Park, J. and Lee, Y.H. (2009a) *MoCRZ1*, a gene encoding a calcineurin-responsive transcription factor, regulates fungal growth and pathogenicity of *Magnaporthe oryzae*. *Fungal Genet. Biol.* **46**, 243–254.

Choi, J.H., Kim, Y. and Lee, Y.H. (2009b) Functional analysis of MCNA, a gene encoding a catalytic subunit of calcineurin, in the rice blast fungus *Magnaporthe oryzae*. *J. Microbiol. Biotechnol.* **19**, 11–16.

Cramer, R.A. Jr., Perfect, B.Z., Pinchai, N., Park, S., Perlin, D.S., Asfaw, Y.G., Heitman, J., Perfect, J.R. and Steinbach, W.J. (2008) Calcineurin target CrzA regulates conidial germination, hyphal growth, and pathogenesis of *Aspergillus fumigatus*. *Eukaryot. Cell*, **7**, 1085–1097.

Cruz, M.C., Fox, D.S. and Heitman, J. (2001) Calcineurin is required for hyphal elongation during mating and haploid fruiting in *Cryptococcus neoformans*. *EMBO J.* **20**, 1020–1032.

da Silva Ferreira, M.E.D.S., Heinekamp, T., Härtl, A., Brakhage, A.A., Semighini, C.P., Harris, S.D., Savoldi, M., de Gouvêa, P.F., Goldman, M.H.D.S. and Goldman, G.H. (2007) Functional characterization of the *Aspergillus fumigatus* calcineurin. *Fungal Genet. Biol.* **44**, 219–230.

Eaton, C.J., Cox, M.P., Ambrose, B., Becker, M., Hesse, U., Schardl, C.L. and Scott, B. (2010) Disruption of signaling in a fungal–grass symbiosis leads to pathogenesis. *Plant Physiol.* **153**, 1780–1794.

Egan, J.D., Garcia-Pedrajas, M.D., Andrews, D.L. and Gold, S.E. (2009) Calcineurin is an antagonist to PKA protein phosphorylation required for postmating filamentation and virulence, while PP2A is required for viability in *Ustilago maydis*. *Mol. Plant–Microbe Interact.* **22**, 1293–1301.

Fortwendel, J.R., Juvvadi, P.R., Pinchai, N., Perfect, B.Z., Alspaugh, J.A., Perfect, J.R. and Steinbach, W.J. (2009) Differential effects of inhibiting chitin and 1,3-β-D-glucan synthesis in Ras and calcineurin mutants of *Aspergillus fumigatus*. *Antimicrob. Agents Chemother.* **53**, 476–482.

Fukuda, K., Yamada, K., Deoka, K., Yamashita, S., Ohta, A. and Horiuchi, H. (2009) Class III chitin synthase ChsB of *Aspergillus nidulans* localizes at the sites of polarized cell wall synthesis and is required for conidial development. *Eukaryot. Cell*, **8**, 945–956.

Green, K.A., Becker, Y., Fitzsimons, H.L. and Scott, B. (2016) An *Epichloë festucae* homologue of MOB3, a component of the STRIPAK complex, is required for the establishment of a mutualistic symbiotic interaction with *Lolium perenne*. *Mol. Plant Pathol.* **17**, 1480–1492.

Green, K.A., Becker, Y., Tanaka, A., Takemoto, D., Fitzsimons, H.L., Seiler, S., Lalucque, H., Silar, P. and Scott, B. (2017) SymB and SymC, two membrane associated proteins, are required for *Epichloë festucae* hyphal cell–cell fusion and maintenance of a mutualistic interaction with *Lolium perenne*. *Mol. Microbiol.* **103**, 657–677.

Hahn, H., McManus, M.T., Warnstorff, K., Monahan, B.J., Young, C.A., Davies, E., Tapper, B.A. and Scott, B. (2008) *Neotyphodium* fungal endophytes confer physiological protection to perennial ryegrass (*Lolium perenne* L.) subjected to a water deficit. *Environ. Exp. Bot.* **63**, 183–199.

Hameed, S., Dhamgaye, S., Singh, A., Goswami, S.K. and Prasad, R. (2011) Calcineurin signaling and membrane lipid homeostasis regulates iron mediated multidrug resistance mechanisms in *Candida albicans*. *PLoS One*, **6**, e18684.

Harel, A., Bercovich, S. and Yarden, O. (2006) Calcineurin is required for sclerotial development and pathogenicity of *Sclerotinia sclerotiorum* in an oxalic acid-independent manner. *Mol. Plant–Microbe Interact.* **19**, 682–693.

Harren, K., Schumacher, J. and Tudzynski, B. (2012) The Ca^{2+}/calcineurin-dependent signaling pathway in the gray mold *Botrytis cinerea*: the role of calcipressin in modulating calcineurin activity. *PLoS One*, **7**, e41761.

Horiuchi, H., Fujiwara, M., Yamashita, S., Ohta, A. and Takagi, M. (1999) Proliferation of intrahyphal hyphae caused by disruption of *csmA*, which encodes a class V chitin synthase with a myosin motor-like domain in *Aspergillus nidulans*. *J. Bacteriol.* **181**, 3721–3729.

Ichinomiya, M., Yamada, E., Yamashita, S., Ohta, A. and Horiuchi, H. (2005) Class I and class II chitin synthases are involved in septum formation in the filamentous fungus *Aspergillus nidulans*. *Eukaryot. Cell*, **4**, 1125–1136.

Itoh, Y., Johnson, R. and Scott, B. (1994) Integrative transformation of the mycotoxin-producing fungus, *Penicillium paxilli*. *Curr. Genet.* **25**, 508–513.

Juvvadi, P.R., Fortwendel, J.R., Rogg, L.E., Burns, K.A., Randell, S.H. and Steinbach, W.J. (2011) Localization and activity of the calcineurin catalytic and regulatory subunit complex at the septum is essential for hyphal elongation and proper septation in *Aspergillus fumigatus*. *Mol. Microbiol.* **82**, 1235–1259.

Juvvadi, P.R., Gehrke, C., Fortwendel, J.R., Lamoth, F., Soderblom, E.J., Cook, E.C., Hast, M.A., Asfaw, Y.G., Moseley, M.A., Creamer, T.P. and Steinbach, W.J. (2013) Phosphorylation of calcineurin at a novel serine–proline rich region orchestrates hyphal growth and virulence in *Aspergillus fumigatus*. *PLoS Pathog.* **9**, e1003564.

Juvvadi, P.R., Pemble, C.W., Ma, Y. and Steinbach, W.J. (2016) Novel motif in calcineurin catalytic subunit is required for septal localization of calcineurin in *Aspergillus fumigatus*. *FEBS Lett.* **590**, 501–508.

Juvvadi, P.R. and Steinbach, W.J. (2015) Calcineurin orchestrates hyphal growth, septation, drug resistance and pathogenesis of *Aspergillus fumigatus*: where do we go from here? *Pathogens*, **4**, 883–893.

Kim, K.W. and Hyun, J.W. (2007) Nonhost-associated proliferation of intrahyphal hyphae of citrus scab fungus *Elsinoe fawcettii*: refining the perception of cell-within-a-cell organization. *Micron*, **38**, 565–571.

Kim, J.E., Lee, H.J., Lee, J., Kim, K.W., Yun, S.H., Shim, W.B. and Lee, Y.W. (2009) *Gibberella zeae* chitin synthase genes, *GzCHS5* and *GzCHS7*, are required for hyphal growth, perithecia formation, and pathogenicity. *Curr. Genet.* **55**, 449–459.

Kraus, P.R., Fox, D.S., Cox, G.M. and Heitman, J. (2003) The *Cryptococcus neoformans* MAP kinase Mpk1 regulates cell integrity in response to antifungal drugs and loss of calcineurin function. *Mol. Microbiol.* **48**, 1377–1387.

Latch, G.C.M. and Christensen, M.J. (1985) Artificial infection of grasses with endophytes. *Ann. Appl. Biol.* **107**, 17–24.

Lee, S.C., Li, A., Calo, S. and Heitman, J. (2013) Calcineurin plays key roles in the dimorphic transition and virulence of the human pathogenic zygomycete *Mucor circinelloides*. *PLoS Pathog.* **9**, e1003625.

Leuchtmann, A., Bacon, C.W., Schardl, C.L., White, J.F. Jr. and Tadych, M. (2014) Nomenclatural realignment of *Neotyphodium* species with genus *Epichloë*. *Mycologia*, **106**, 202–215.

Li, F., Wang, Z.L., Zhang, L.B., Ying, S.H. and Feng, M.G. (2015) The role of three calcineurin subunits and a related transcription factor (Crz1) in conidiation, multistress tolerance and virulence in *Beauveria bassiana*. *Appl. Microbiol. Biotechnol.* **99**, 827–840.

Miller, J.H. (1972) *Experiments in Molecular Genetics*. New York: Cold Spring Harbour Laboratory Press.

Moon, C.D., Scott, B., Schardl, C.L. and Christensen, M.J. (2000) The evolutionary origins of *Epichloë* endophytes from annual ryegrasses. *Mycologia*, **92**, 1103–1118.

Moon, C.D., Tapper, B.A. and Scott, B. (1999) Identification of *Epichloë* endophytes in planta by a microsatellite-based PCR fingerprinting assay with automated analysis. *Appl. Environ. Microbiol.* **65**, 1268–1279.

Munro, C.A., Selvaggini, S., de Bruijn, I., Walker, L., Lenardon, M.D., Gerssen, B., Milne, S., Brown, A.J. and Gow, N.A. (2007) The PKC, HOG and Ca^{2+} signalling pathways co-ordinately regulate chitin synthesis in *Candida albicans*. *Mol. Microbiol.* **63**, 1399–1413.

Muszkieta, L., Aimanianda, V., Mellado, E., Gribaldo, S., Alcàzar-Fuoli, L., Szewczyk, E., Prevost, M.-C. and Latgé, J.-P. (2014) Deciphering the role of the chitin synthase families 1 and 2 in the *in vivo* and *in vitro* growth of *Aspergillus fumigatus* by multiple gene targeting deletion. *Cell Microbiol.* **16**, 1784–1805.

Odom, A., Muir, S., Lim, E., Toffaletti, D.L., Perfect, J. and Heitman, J. (1997) Calcineurin is required for virulence of *Cryptococcus neoformans*. *EMBO J.* **16**, 2576–2589.

Oliveira-Garcia, E. and Deising, H.B. (2016) The glycosylphosphatidylinositol anchor biosynthesis genes *GPI12*, *GAA1*, and *GPI8* are essential for cell-wall integrity and pathogenicity of the maize anthracnose fungus *Colletotrichum graminicola*. *Mol. Plant–Microbe Interact.* **29**, 889–901.

Prokisch, H., Yarden, O., Dieminger, M., Tropschug, M. and Barthelmess, I.B. (1997) Impairment of calcineurin function in *Neurospora crassa* reveals its essential role in hyphal growth, morphology and maintenance of the apical Ca^{2+} gradient. *Mol. Gen. Genet.* **256**, 104–114.

Rasmussen, C., Garen, C., Brining, S., Kincaid, R.L., Means, R.L. and Means, A.R. (1994) The calmodulin-dependent protein phosphatase catalytic subunit (calcineurin A) is an essential gene in *Aspergillus nidulans*. *EMBO J.* **13**, 3917–3924.

Rumi-Masante, J., Rusinga, F.I., Lester, T.E., Dunlap, T.B., Williams, T.D., Dunker, A.K., Weis, D.D. and Creamer, T.P. (2012) Structural basis for activation of calcineurin by calmodulin. *J. Mol. Biol.* **415**, 307–317.

Rusnak, F. and Mertz, P. (2000) Calcineurin: form and function. *Physiol. Rev.* **80**, 1483–1521.

Sanglard, D., Ischer, F., Marchetti, O., Entenza, J. and Bille, J. (2003) Calcineurin A of *Candida albicans*: involvement in antifungal tolerance, cell morphogenesis and virulence. *Mol. Microbiol.* **48**, 959–976.

Schardl, C.L., Leuchtmann, A. and Spiering, M.J. (2004) Symbioses of grasses with seedborne fungal endophytes. *Annu. Rev. Plant Biol.* **55**, 315–340.

**Schardl, C.L., Young, C.A., Hesse, U., Amyotte, S.G., Andreeva, K., Calie, P.J., Fleetwood, D.J., Haws, D.C., Moore, N., Oeser, B., Panaccione, D.G., Schweri, K.K., Voisey, C.R., Farman, M.L., Jaromczyk, J.W., Roe, B.A., O'Sullivan, D.M., Scott, B., Tudzynski, P., An, Z., Arnaoudova, E.G., Bullock, C.T., Charlton, N.D., Chen, L., Cox, M., Dinkins, R.D., Florea, S., Glenn, A.E., Gordon, A., Güldener, U., Harris, D.R., Hollin, W., Jaromczyk, J., Johnson, R.D., Khan, A.K., Leistner, E., Leuchtmann, A., Li, C., Liu, JGe., Liu, J., Liu, M., Mace, W., Machado, C., Nagabhyru, P., Pan, J., Schmid, J., Sugawara, K., Steiner, U., Takach, J.E., Tanaka, E., Webb, J.S., Wilson, E.V., Wiseman, J.L., Yoshida, R. and Zeng, Z. (2013) Plant-symbiotic fungi as chemical engineers: multi-genome analysis of the Clavicipitaceae reveals dynamics of alkaloid loci. *PLoS Genet.* 9, e1003323.

Schumacher, J., de Larrinoa, I.F. and Tudzynski, B. (2008) Calcineurin-responsive zinc finger transcription factor CRZ1 of *Botrytis cinerea* is required for growth, development, and full virulence on bean plants. *Eukaryot. Cell*, **7**, 584–601.

Scott, B. (2001) *Epichloë* endophytes: fungal symbionts of grasses. *Curr. Opin. Microbiol.* **4**, 393–398.

Spiers, A.G. and Hopcroft, D.H. (1993) Black canker and leaf spot of Salix in New Zealand caused by *Glomerella miyabeana* (*Colletotrichum gloeosporioides*). *Eur. J. Forest Pathol.* **23**, 92–102.

Steinbach, W.J., Cramer, R.A. Jr., Perfect, B.Z., Asfaw, Y.G., Sauer, T.C., Najvar, L.K., Kirkpatrick, W.R., Patterson, T.F., Benjamin, D.K. Jr., Heitman, J. and Perfect, J.R. (2006) Calcineurin controls growth, morphology, and pathogenicity in *Aspergillus fumigatus*. *Eukaryot. Cell*, **5**, 1091–1103.

Stie, J. and Fox, D. (2008) Calcineurin regulation in fungi and beyond. *Eukaryot. Cell*, **7**, 177–186.

Takemoto, D., Tanaka, A. and Scott, B. (2006) A p67Phox-like regulator is recruited to control hyphal branching in a fungal–grass mutualistic symbiosis. *Plant Cell*, **18**, 2807–2821.

Takeshita, N., Yamashita, S., Ohta, A. and Horiuchi, H. (2006) *Aspergillus nidulans* class V and VI chitin synthases CsmA and CsmB, each with a myosin motor-like domain, perform compensatory functions that are essential for hyphal tip growth. *Mol. Microbiol.* **59**, 1380–1394.

Tanaka, A., Christensen, M.J., Takemoto, D., Park, P. and Scott, B. (2006) Reactive oxygen species play a role in regulating a fungus–perennial ryegrass mutualistic interaction. *Plant Cell*, **18**, 1052–1066.

Tanaka, A., Takemoto, D., Hyon, G.S., Park, P. and Scott, B. (2008) NoxA activation by the small GTPase RacA is required to maintain a mutualistic symbiotic association between *Epichloë festucae* and perennial ryegrass. *Mol. Microbiol.* **68**, 1165–1178.

Tanaka, A., Tapper, B.A., Popay, A., Parker, E.J. and Scott, B. (2005) A symbiosis expressed non-ribosomal peptide synthetase from a mutualistic fungal endophyte of perennial ryegrass confers protection to the symbiotum from insect herbivory. *Mol. Microbiol.* **57**, 1036–1050.

Thewes, S. (2014) Calcineurin-Crz1 signaling in lower eukaryotes. *Eukaryot. Cell*, **13**, 694–705.

Viaud, M., Brunet-Simon, A., Brygoo, Y., Pradier, J.M. and Levis, C. (2003) Cyclophilin A and calcineurin functions investigated by gene inactivation, cyclosporin A inhibition and cDNA arrays approaches in the phytopathogenic fungus *Botrytis cinerea*. *Mol. Microbiol.* **50**, 1451–1465.

Walker, L.A., Lee, K.K., Munro, C.A. and Gow, N.A. (2015) Caspofungin treatment of *Aspergillus fumigatus* results in ChsG-dependent upregulation of chitin synthesis and the formation of chitin-rich microcolonies. *Antimicrob. Agents Chemother.* **59**, 5932–5941.

Werner, S., Sugui, J.A., Steinberg, G. and Deising, H.B. (2007) A chitin synthase with a myosin-like motor domain is essential for hyphal growth, appressorium differentiation, and pathogenicity of the maize anthracnose fungus *Colletotrichum graminicola*. *Mol. Plant–Microbe Interact.* **20**, 1555–1567.

Young, C.A., Bryant, M.K., Christensen, M.J., Tapper, B.A., Bryan, G.T. and Scott, B. (2005) Molecular cloning and genetic analysis of a symbiosis-expressed gene cluster for lolitrem biosynthesis from a mutualistic endophyte of perennial ryegrass. *Mol. Genet. Genomics*, **274**, 13–29.

Zhang, H., Zhao, Q., Liu, K., Zhang, Z., Wang, Y. and Zheng, X. (2009) MgCRZ1, a transcription factor of *Magnaporthe grisea*, controls growth, development and is involved in full virulence. *FEMS Microbiol. Lett.* **293**, 160–169.

SUPPORTING INFORMATION

Additional Supporting Information may be found in the online version of this article at the publisher's website:

Fig. S1 *cnaA* copy number varies amongst strains of *Epichloë* species. (a) Autoradiograph of DNA blot of *Bam*HI genomic digests of *E. festucae* strains. (b) Autoradiograph of DNA blot of *Bam*HI genomic digests of *Epichloë* species, including *Epichloë elymi* (WWG1, WWG3, E184), *Epichloë brachyelytri* (E1040, E1124), *Epichloë bromicola* (E501, E799), *Epichloë baconii* (E424), *Epichloë typhina* (E425 and E505) and *Epichloë typhina* ssp. *poae* (E1022). Both DNA blots were probed with a [^{32}P]-labelled *cnaA2*-containing polymerase chain reaction (PCR) fragment that was generated with primers 1372-2F and 1372-5R using *E. festucae* E2368 genomic DNA as the template. This probe was expected to hybridize to *Bam*HI fragments of 8.8, 5.9 and 1.3 kb in *E. festucae* E2368. Four strains of *E. festucae* (E189, E2368, Fr1, 1035.33) showed the expected hybridization pattern (*). However, three strains of other *Epichloë* spp. (WWG1, WWG3, E424) showed a similar, but not identical, pattern of hybridization (#). A difference in the size of the largest hybridization band present in *E. elymi* strains, as well as the absence of the two largest bands in *E. baconii*, suggest deletions in these genomes.

Fig. S2 Deletion of *Epichloë festucae* Fl1 *cnaA*. (a) Physical map of the *cnaA* wild-type (WT) genomic region, linear insert of *cnaA* deletion construct pMMI4 and *cnaA* complementation construct pMMI11, showing restriction enzyme sites for *Pst*I (P), *Bam*HI (B), *Eco*RI (E), *Eco*RV (EV), *Hin*dIII (H) and *Nde*I (N). (b) Autoradiograph of a Southern blot of *Nde*I genomic DNA digests of *E. festucae* Fl1 wild-type (WT) and *cnaA* deletion strains (Δ*cnaA*), probed with [^{32}P]-labelled pMMI4. The expected sizes of the fragments are shown.

Fig. S3 Remediation of *Epichloë festucae* Fl1 Δ*cnaA* culture phenotype. Remediation of the Δ*cnaA* culture phenotype (secretion of yellow pigment) observed when a plug of the mutant was grown on potato dextrose agar (PDA) by spreading ground mycelia on PDA or by subculture of a plug of the mutant on PDA supplemented with $MgCl_2$.

Fig. S4 Deletion of *Epichloë festucae* E2368 *cnaA1* and *cnaA2*. (a) Physical map of the *cnaA1* wild-type (WT) genomic region, linear insert of *cnaA* replacement construct pMMI4, showing restriction enzyme sites for *Pst*I (P), *Bam*HI (B), *Eco*RI (E), *Eco*RV (EV) and *Hin*dIII (H). The arrowheads indicate the primers used for screening of the replacement event. (b) Polymerase chain reaction (PCR) products of the expected size generated with the primer pair MI13 and MI14, specific for *cnaA1*. (c) Physical map of the *cnaA2* wild-type (WT) genomic region, linear insert of *cnaA2* deletion construct pMMI13 and *cnaA2* complementation construct pMMI12, used to complement the *E. festucae* Fl1 Δ*cnaA* strain. The arrowheads indicate the primers used for preparation of the deletion and complementation constructs and for screening of the replacement event. (d) PCR products of the expected size generated with primer pair MI15 and MI16, specific for *cnaA2*.

Table S1 Calcineurin A-encoding genes in sequenced *Epichloë* genomes.

Table S2 Biological material.

Table S3 Primers used in this study.